



Formation of an array of isolated alumina nanotubes

To cite this article: Y. F. Mei *et al* 2003 *EPL* **62** 595

View the [article online](#) for updates and enhancements.

Related content

- [Microstructural Models of Alumina Nanotubes and Anodic Porous Alumina Film Formed in Sulphuric Acid](#)
Pu Lin, Chen Zhi-Qiang, Tan Chao *et al.*
- [Self-organized formation of hexagonal nanopore arrays in anodic alumina](#)
Zhou Wei-ya, Li Yu-bao, Liu Zu-qin, Tang Dong-sheng *et al.*
- [Fabrication of anodic aluminium oxide templates on curved surfaces](#)
Aijun Yin, Rodney S Guico and Jimmy Xu

Recent citations

- [Hybrid pulse anodization for the fabrication of porous anodic alumina films from commercial purity \(99%\) aluminum at room temperature](#)
C K Chung *et al*
- [In situ fabrication of alumina nanotube array and photoluminescence](#)
G. S. Huang
- [Alumina nanotubes and nanowires from Al-based porous alumina membranes](#)
M. Jiang *et al*

Formation of an array of isolated alumina nanotubes

Y. F. MEI¹, X. L. WU¹(*), X. F. SHAO¹, G. G. SIU² and X. M. BAO¹

¹ *National Laboratory of Solid State Microstructures and Department of Physics Nanjing University - Nanjing 210093, PRC*

² *Department of Physics and Materials Science, City University of Hong Kong Kowloon, Hong Kong, PRC*

(received 19 December 2002; accepted in final form 12 March 2003)

PACS. 82.45.-h – Electrochemistry and electrophoresis.

PACS. 81.20.-n – Methods of materials synthesis and materials processing.

PACS. 81.07.De – Nanotubes.

Abstract. – An ordered array of isolated alumina nanotubes was obtained using an anodizing method of Si-based Al films, which was composed of three steps: anodization of a Si-based Al film under a constant dc voltage in sulfuric acid to form a porous alumina film, followed by further anodization under a pulse voltage for a short time to detach the alumina film from the Si substrate, and final immersion of the alumina film into dilute phosphoric acid for a few minutes to form an ordered nanotube array. This kind of ordered arrays is expected to have important applications as templates in fabricating ordered nanostructures.

Recently, much attention has been paid to fabrications of microtubes [1] and nanotubes [2,3] because of their potential applications in drug delivery [4], bioencapsulation [5], probes in scanning probe microscopy [6], and hydrogen storage [7]. For example, straight carbon nanotubes have been fabricated and used in single-electron devices [8] and field-effect transistors [9]. Y-junction carbon nanotubes have been fabricated for seeking important applications in nanoelectronics [10]. To explore significant usage in field emission display and data storage [11], highly ordered carbon nanotube arrays [12] and other ordered nanostructures [13–17] have also been produced using anodic porous alumina (APA) templates. In the literature [3], we reported the synthesis of individual alumina nanotubes (ANTs) by employing electrochemical etching of Si-based Al films. Some useful features of the ANTs were disclosed. However, it will be significant to fabricate an array of ANTs, because through this array we could not only fabricate a carbon nanotube array but also seek various applications related to the ordered array in nanoelectronics such as fabricating nanocables. In this letter, we report the formation of an ordered array of isolated ANTs using an anodizing method of Si-based Al films under a pulse voltage and with post-processing in dilute phosphoric acid.

Previously, we have presented the fabrication of individual ANTs using two kinds of anodizing methods of Si-based Al films [3]. The current work is still based on our previous experiments. The substrates used in the work were *p*-type (100)-oriented silicon wafers with a resistivity of 5 Ω /cm. Using electron beam evaporation, a layer of Al film with a purity of 99.99% and a thickness of 440 nm was deposited onto the Si wafer to form an Al/Si system. The thickness of the Al film can easily be controlled by changing deposition time. This corresponds to controlling the length of the formed ANTs. Anodization with a platinum plate

(*) E-mail: hkx1wu@nju.edu.cn

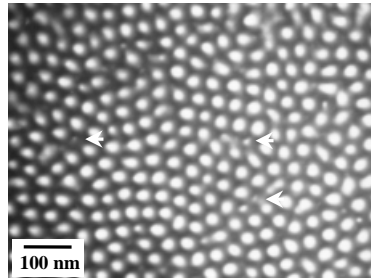


Fig. 1 – TEM image of a Si-based APA film. This film was firstly obtained from step 1, followed by immersion into 5 wt.% phosphoric acid for about 5 min.

as cathode and the Al/Si system as anode was carried out in 15 wt.% sulfuric acid under a constant dc voltage of 40 V. The temperature of the electrolyte was set at room temperature (about 27 °C). The anodization process of the Al/Si system was monitored through the current-time ($I-t$) curve. If the anodization is formed until the APA film is detached from the silicon substrate, we shall call this process step 1.

Figure 1 shows the transmission electron microscope (TEM) image of a Si-based APA film (using a Hitachi H-800-NA microscope operated at 200 keV). This film was firstly obtained from step 1, followed by immersion in 5 wt.% phosphoric acid for about 5 min. The post-processing leads to the enlargement of the nanopore diameters. It can be seen from the TEM image that the nanopore arrangement is uniform and ordered, displaying a hexagonal symmetry. The mean diameter of nanopores is about 25 nm. The interpore distance is about 45 nm. This interpore distance may cause a suspicion: Typically, it should be 2.5 nm/V. Therefore, the applied voltage of 40 V should produce an interpore distance of about 100 nm. This is inconsistent with our experimental result. In fact, this can be explained from the sample difference. In our Al/Si system, on the onset of anodization, the potential applied to the Al film is 40 V, thus the current has a large value ($> 18 \text{ mA/cm}^2$). This can be seen from the $I-t$ curve. However, after an unstable growth of less than 20 s, the Si substrate shares a partial applied voltage. This is accompanied by a decrease of the current ($\approx 10 \text{ mA/cm}^2$). Therefore, the potential applied to the Al film is eventually lower than 40 V, possibly $\sim 20 \text{ V}$. The applied voltage of 20 V can result in an interpore distance of $\sim 45 \text{ nm}$. The TEM result implies that if we could obtain isolated ANTs, their arrangement would also be ordered.

To form an array of isolated ANTs, we made use of experimental parameters and configuration similar to those of step 1, but the anodization was stopped (by turning off the current) at the moment when the Si wafer just starts to be anodized and the Al film has completely been anodized. Subsequent anodization was continued for a short time (1-5 s) under a pulse voltage ($V_{\text{max}} = 40 \text{ V}$, $V_{\text{min}} = 0 \text{ V}$, $f = 1 \text{ Hz}$) until the detachment of the APA film from the Si substrate. We call this process step 2. After step 2, the detached APA film was immersed into a 5 wt.% phosphoric acid solution at 27 °C for 5-10 minutes and followed by TEM observations.

Figure 2(a) displays the TEM image of an array of isolated ANTs. The barrier layer at the bottom of the APA film has been dissolved by phosphoric acid. Therefore, the isolated ANTs are punch-through and separated from each other. They are basically packed hexagonally (see the circular area). Each of the isolated ANTs looks like a wheel, having different diameters. The mean outer and inner diameters were calculated to be about 40 and 20 nm, respectively. Some small ANTs can also be observed (by the short arrows), which correspond to the minute

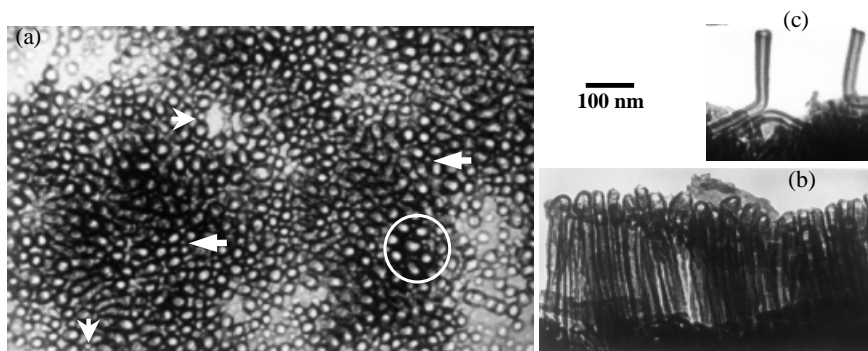


Fig. 2 – (a) TEM image of an array of isolated ANTs. The short and long arrows indicate the minute ANTs and voids at triple points, respectively. (b) TEM image of a row of isolated ANTs slightly tilted. (c) TEM image of the separated ANTs with twist angle of about 75° .

pores in the APA film formed in step 1 (see the arrows in fig. 1). This indicates that the isolated ANT array is closely related to the APA film with highly ordered nanopore arrangement. The origin of the minute nanopores (or ANTs) is considered to be impurity(or defect)-induced in the deposited Al film or to be the merged pores during the competitive growth of the cells [18]. Before the merged pores vanish, the anodization process has already finished due to the short anodic time. In our experiment, the anodic time was set to be 4 min, which is far away from the stable competing growth of the APA film on bulk Al. So the merged pores have small diameters.

A cross-sectional TEM image of a row of isolated ANTs is shown in fig. 2(b). These ANTs are separated from the array. They are not completely straight, showing a slight bend. However, we can see from fig. 2(a) that the ANTs in the array are basically straight. This result indicates that the isolated ANTs have fine flexibility. This result can further be seen from fig. 2(c), which shows two split ANTs with twist angles of about 75° . In addition, an ANT bent up to 90° can also be observed in fig. 2(c). This property can be expected to have important applications in fabricating nanocables capable of a twist rotation up to 90° .

Individual ANTs can also be obtained in this experiment, but their formation mechanism is different from that of the array of isolated ANTs. Many fracture morphologies (the cleavage features) that look like a spider web, a screw thread, and concentric circles often appear in the APA film that leads to individual ANTs [3], but they do not appear in the APA film that leads to an array of isolated ANTs. The highly ordered arrangement of nanopores in the current APA film is another feature, which cannot be observed in the APA film only for forming individual ANTs. Hence, the cleavage regions and highly disordered arrangement of nanopores, described in the previous literature [3], may not be the main reasons for inducing the ANTs. Other factors such as the voids at triple points between cells, the Al/Si interface, and the applied pulse voltage (it was especially adopted for the formation of the array of isolated ANTs) may play an important role.

Voids located at triple points between cells can clearly be observed in fig. 2(a) (by the long arrows), which also appear in the film only for forming individual ANTs. They were considered to be responsible for the cleavage of the D-D route (see fig. 3) that induces the formation of nanotubes [3]. Four typical cleavage routes of the APA film were discussed in the previous literature [19]. For the A-A, B-B, and C-C routes, they have nothing to do with the formation of individual ANTs. Obviously, if two or more D-D cleavages interlace around

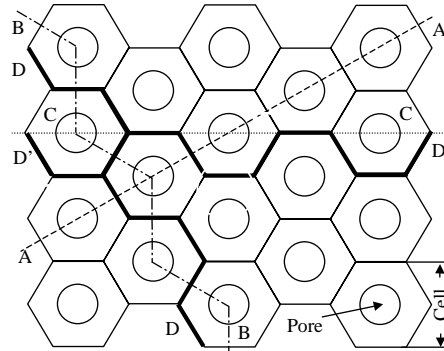


Fig. 3 – Four typical cleavage models of the APA film: A-A, B-B, C-C, and D-D routes. The D-D cleavages interlaced around some cells are responsible for the ANTs.

some cells, perfect ANTs can be obtained from the detached APA film due to tensile stress. When a pulse voltage is applied to the Si-based APA film, tensile stress on the film makes these potential nanotubes separate from each other and thus an array of isolated ANTs is formed. As for the Al/Si interface, we cannot affirm that mismatching between the Al film and Si substrate directly induces the formation of both individual ANTs and the isolated ANT array. However, we believe that it should play an important role, because no ANTs were found in the APA film on bulk Al.

To check the microstructural characteristics of the Al/Si system, we carried out a TEM observation on the Al film deposited on the Si substrate. The experimental result shows that the Al film is composed of polycrystalline Al (see fig. 4(a)). Small Al grains with sizes of 100–1000 nm are closely packed together. The grain sizes change with the thickness of the deposited Al film. In addition, the existence of grain boundaries is very clear. After an anodic treatment with formation of the ANT array, the APA film shows some regions without the ANTs (see fig. 4(b)). This is due to the detachment of partial ANTs from the substrate. Figure 4(b) also shows some nanopores arranged in line. The positions of these lines correspond to the boundaries of Al grains. The phenomenon arises from the difference in the growth speed of the nanopores. During the growth of the nanopores, pore formation along the grain boundary is faster than that inside the grain, because the grain boundary generally provides concaves [12]. These pores pass fast through the barrier layer and thus

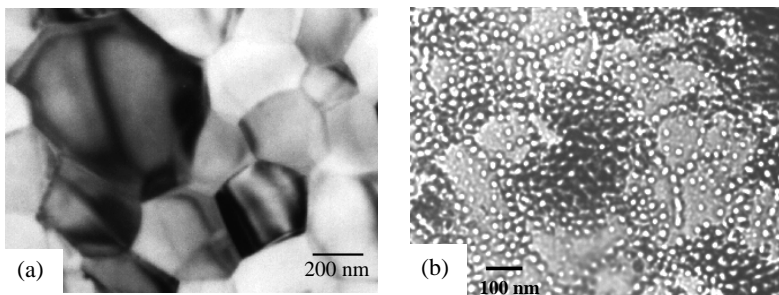


Fig. 4 – Planar TEM images of (a) an Al film deposited on the Si substrate (the Al/Si system) and (b) a Si-based APA film with the ANTs removed partially.

show large pore diameters. At the same time, since different regions have different growth speeds of nanopores, the tensile stress will fluctuate and therefore causing the formation of ANTs with different diameters. With a pulse voltage further applied on the film, the ANTs are separated from each other and an ANT array is finally formed.

In conclusion, an ordered array of isolated ANTs has been obtained using an anodizing method of Si-based Al films. The investigations on the structure and cleavage properties of the APA film give some clues to the self-organized growth mechanism of porous alumina. Our results provide a possibility for synthesising ordered metal and semiconductor nanostructures with peculiar optical and electric properties through the array of isolated ANTs.

* * *

This work was supported by Grants (Nos. 10225416 and BK2002077) from the Natural Science Foundations of China and JiangSu province. Partial support was from the Trans-Century Training Programme Foundation for the Talents by the State Education Commission and the Major State Basic Research Project No. G001CB3095 of China.

REFERENCES

- [1] MARTIN C. R., *Science*, **266** (1994) 1961, and references therein.
- [2] IJIMA S., *Nature*, **354** (1991) 56; SPAHR M. E., BITTERLI P., NESPER R., MÜLLER M., KRUMEICH F. and NISSEN H. U., *Angew. Chem. Int. Ed.*, **14** (1998) 3160.
- [3] PU L., BAO X. M., ZOU J. P. and FENG D., *Angew. Chem. Int. Ed.*, **40** (2001) 1490.
- [4] GREF R., MINAMITAKE Y., PERACCHIA M. T., TRUBETSKOY V., TORCHILIN V. and LANGER R., *Science*, **263** (1994) 1600.
- [5] PARTHASARATHY R. and MARTIN C. R., *Nature*, **369** (1994) 298.
- [6] KYOTANI T., TSAI L. and TOMITA A., *Chem. Mater.*, **8** (1996) 2190.
- [7] LIU C., YAN F., LIU M., CONG H. T., CHENG H. M. and DRESSELHAUS M. S., *Science*, **286** (1999) 1127; SCHLAPBACH L. and ZÜTTEL A., *Nature*, **414** (2001) 353.
- [8] TANS S. J., DEVORET M. H., DAI H. J., THESS A., SMALLEY R. E., GEERLIGS L. J. and DEKKER C., *Nature (London)*, **386** (1997) 474.
- [9] TANS S. J., VERSCHUEREN A. R. M. and DEKKER C., *Nature (London)*, **393** (1998) 49.
- [10] LI J., PAPADOPOULOS C. and XU J. M., *Nature (London)*, **402** (1999) 253; PAPADOPOULOS C., RAKITIN A., LI J., VEDENEV A. S. and XU J. M., *Phys. Rev. Lett.*, **85** (2000) 3476.
- [11] ROUTKEVITCH D., TAGER A. A., HARUYAMA J., ALMAWLAWI D., MOSKOVITS M. and XU J. M., *IEEE Trans. Electron Devices*, **43** (1996) 1646, and reference therein; TONUCCI R. J., JUSTUS B. L., CAMPILLO A. J. and FORD C. E., *Science*, **258** (1992) 783.
- [12] MASUDA H. and FUKUDA K., *Science*, **268** (1995) 1466.
- [13] NIELSCH K., MÜLLER F., LI A. P. and GÖSELE U., *Adv. Mater.*, **8** (2000) 582.
- [14] CHU S. Z., WADA K., INOUE S., TODOROKI S., TAKAHASHI Y. K. and HONO K., *Chem. Mater.*, **14** (2002) 4595; CHU S. Z., WADA K., INOUE S. and TODOROKI S., *J. Electrochem. Soc.*, **149** (2002) B321.
- [15] CROUSE D., LO Y., MILLER A. E. and CROUSE M., *Appl. Phys. Lett.*, **76** (2000) 49.
- [16] SUN Z. J. and KIM H. K., *Appl. Phys. Lett.*, **81** (2002) 3458.
- [17] MASUDA H., YASUI K., SAKAMOTO Y., NAKAO M., TAMAMURA T. and NISHIO K., *Jpn. J. Appl. Phys.*, **40** (2001) L1267.
- [18] THOMPSON G. E., *Thin Solid Films*, **297** (1997) 192.
- [19] BOOKER C. and BRIT J. L., *J. Appl. Phys.*, **8** (1957) 347; BAILEY G. and WOOD G. C., *Trans. Inst. Met. Finish.*, **52** (1974) 187.